ChemPubSoc Europe

DOI: 10.1002/cphc.201501118

CHEMPHYSCHEM Articles

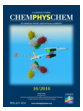

Absolute Configuration from Different Multifragmentation Pathways in Light-Induced Coulomb Explosion Imaging

Martin Pitzer,[a] Gregor Kastirke,[a] Maksim Kunitski,[a] Till Jahnke,[a] Tobias Bauer,[a] Christoph Goihl,[a] Florian Trinter,[a] Carl Schober,[a] Kevin Henrichs,[a] Jasper Becht,[a] Stefan Zeller,[a] Helena Gassert,[a] Markus Waitz,[a] Andreas Kuhlins,[a] Hendrik Sann,[a] Felix Sturm,[a] Florian Wiegandt,[a] Robert Wallauer,[a] Lothar Ph. H. Schmidt,[a] Allan S. Johnson,[b] Manuel Mazenauer,[c] Benjamin Spenger,[c] Sabrina Marquardt,[d] Sebastian Marquardt,[d] Horst Schmidt-Böcking,[a] Jürgen Stohner,[c] Reinhard Dörner,[a] Markus Schöffler,*[a] and Robert Berger*[d]

The absolute configuration of individual small molecules in the gas phase can be determined directly by light-induced Coulomb explosion imaging (CEI). Herein, this approach is demonstrated for ionization with a single X-ray photon from a synchrotron light source, leading to enhanced efficiency and faster fragmentation as compared to previous experiments with a femtosecond laser. In addition, it is shown that even incomplete fragmentation pathways of individual molecules from a racemic CHBrClF sample can give access to the absolute configuration in CEI. This leads to a significant increase of the applicability of the method as compared to the previously reported complete break-up into atomic ions and can pave the way for routine stereochemical analysis of larger chiral molecules by light-induced CEI.

1. Introduction

Determination of the absolute configuration of a chiral species is a keystone of stereochemistry. The direct assignment of absolute configuration in crystalline samples is routinely performed with Bijvoet's method, which employs anomalous diffraction of X-rays.[1] For a vast range of substances that cannot easily be crystalized, determination of absolute configuration requires knowledge of the handedness of related compounds or extensive theoretical models. Recently, two research teams[2,3] have shown independently the use of Coulomb explosion imaging (CEI)[4] for the direct determination of absolute configuration of small chiral molecules in the gas phase.

When the bonding electrons are removed from a molecule instantaneously, the resulting atomic cations, which essentially remain in their equilibrium positions during ionization, experience strongly repelling Coulombic forces. The molecule subsequently undergoes a so-called Coulomb explosion. By performing a coincident measurement of the fragment ions' linear momenta, the microscopic structure of the molecule is imaged on the macroscopic detection device. For very small systems, Coulomb explosion imaging is capable of visualizing even fine details such as the nodal structure of the wavefunction[5] or the tunneling part of loosely bound helium molecules.[6,7]

First investigations on the structure of the CH_4^+ ion were already carried out in 1986 with foil-induced Coulomb explosion imaging.[8] In this approach, the molecular ions are accelerated and sent through a thin foil, stripping off the electrons. Kitamura et al.[9] employed highly charged argon atoms to multiply ionize perdeuterated methane CD_4 to demonstrate the dynamic chirality of this molecule. Herwig et al.[3,10] used foil-induced Coulomb explosion imaging to determine the absolute configuration of the monocation of 1,2-dideutero-oxirane. This approach, however, is limited to relatively small masses. Pitzer et al.[2] have employed a high-power Ti:sapphire femtosecond laser system with high repetition rate for the multiple ionization of CHBrClF (from a racemic mixture) and Cold Target Recoil Ion Momentum Spectroscopy (COLTRIMS)[11] for the detection of fragments. The results show that unambiguous de-

[a] Dr. M. Pitzer, G. Kastirke, Dr. M. Kunitski, Dr. T. Jahnke, Dr. T. Bauer, C. Goihl, F. Trinter, C. Schober, K. Henrichs, J. Becht, S. Zeller, H. Gassert, M. Waitz, A. Kuhlins, H. Sann, F. Sturm, F. Wiegandt, Dr. R. Wallauer, Dr. L. Ph. H. Schmidt, Prof. Dr. H. Schmidt-Böcking, Prof. Dr. R. Dörner, Dr. M. Schöffler
Institute for Nuclear Physics
Johann-Wolfgang-Goethe-Universität Frankfurt
Max-von-Laue-Straße 1, 60438 Frankfurt (Germany)
E-mail: schoeffler@atom.uni-frankfurt.de

[b] A. S. Johnson
University of Ottawa
Ottawa, ON, K1N 6N5 (Canada)

[c] M. Mazenauer, B. Spenger, Prof. Dr. J. Stohner
Institute of Chemistry and Biological Chemistry
Zurich University of Applied Sciences, Campus Reidbach
Einsiedlerstrasse 31, 8820 Wädenswil (Switzerland)

[d] S. Marquardt, S. Marquardt, Prof. Dr. R. Berger
Fachbereich Chemie
Philipps-Universität Marburg
Hans-Meerwein-Straße, 35032 Marburg (Germany)
E-mail: robert.berger@uni-marburg.de

Supporting Information for this article can be found under http://dx.doi.org/10.1002/cphc.201501118.

© 2016 Wiley-VCH Verlag GmbH & Co. KGaA, Weinheim

termination of absolute configuration is possible on the level of individual molecules from a racemic mixture. Limitations of laser-induced Coulomb explosion imaging for larger covalently bound systems have been discussed in Ref. [2]. Amongst those is the demand for a comparatively large amount of sample and the timescale of the laser-induced ionization. The latter leads in some cases, for example, for fast moving atoms such as hydrogen, to a broadening of the measured linear momentum distribution.

In this work, we show that a single X-ray photon (with energy $h\nu = 710$ eV) from a synchrotron light source can also be used to induce Coulomb explosion of CHBrClF into up to five atomic ions. First, we discuss the mechanisms contributing to the multiple ionization of the target molecule. We then demonstrate on the level of individual molecules from a racemic mixture the determination of absolute configuration for the complete fragmentation into five singly charged ions and compare the results to those previously obtained in laser experiments. This is followed by an investigation of partial break-ups of the target molecule, that is, break-ups including molecular ions like CH^+. Finally, the advantages and drawbacks of using events with an incomplete detection of the fragments are discussed.

2. Results and Discussion

2.1. Multiple Ionization Induced by a Single X-ray Photon

Once an electron is removed from an inner shell of an atom or a molecule, the excited system will relax to its ground state. An important relaxation process is the Auger decay, during which the excitation energy is transferred to another electron that can escape into the continuum, leaving a doubly charged atom or molecule behind.

With sufficient energy this process can occur in a cascade, leading to multiple ionization. Using photon energies slightly above the ionization threshold of the F(1s) state ($E_B = 688$ eV for atomic fluorine),[12] we observed fragmentation of CHBrClF into up to five singly charged ions.

In order to shed light on the ionization processes involved, we compared our findings to the extensive literature on multiple ionization of the rare-gas atoms from the same row of the periodic table as the halogen atoms in our sample, that is, neon (corresponding to fluorine), argon (corresponding to chlorine) and krypton (corresponding to bromine). All three halogens have energy levels that contribute to the photoionization cross section at the chosen photon energy of 710 eV (see Table 1 in the Supporting Information). As efficient Auger cascades leading to five-fold ionization have been reported for ionization of the krypton 3p or 3d states,[13,14] we expect excitation of the respective bromine state to be the prominent channel. For the four-fold ionization, the chlorine 2s state is expected to play an important role as well.[15,14] Recently, ultrafast charge rearrangement in a similar molecule, CH_3SeH, upon excitation of the Se L-shell by an X-ray free-electron laser has proven to be highly efficient.[16] A further efficient channel for additional charge removal besides Auger decay is the direct photoemission of electron pairs by shake-off or knock-off, known in atoms[17] and molecules.[18] The interplay between the different possibilities for photoionization and the various decay channels for the respective core holes makes it impossible to identify the exact ionization mechanism for single events.

Compared to the previous laser experiment, efficiency is increased significantly. Whereas the fraction of the five-fold fragmentation on the number of total events in the laser experiment was around 5×10^{-6}, it was increased in the synchrotron experiment by more than one magnitude to 7×10^{-5}.

2.2. Complete Fragmentation and Determination of Absolute Configuration

In analogy to our previous work,[2] we first investigate the break-up of CHBrClF into five singly charged ions. The occurrence of this fragmentation pathway can already be seen in the raw photo-ion coincidence spectra (Figure 1). In this graph, sums of the times-of-flight of several particles are plotted; due to linear momentum conservation, ions originating from the same molecule arrange on a line in this plot.

For details on the extraction of the ion momenta from the experimental data, we refer to the Experimental Section. By checking whether linear momentum conservation is fulfilled for a certain assignment, the correct isotopic mass is identified. Furthermore, this test allows to eliminate false coincidences and thus increase the signal-to-noise-ratio. For the remaining events, several triple products can be calculated from the linear momentum vectors of the respective three ions. In Figure 2a, we show the chirality parameter $\cos\theta_{F\cdot(Cl\times Br)} = \vec{p}_F \cdot (\vec{p}_{Cl} \times \vec{p}_{Br}) \cdot (|\vec{p}_F||\vec{p}_{Cl} \times \vec{p}_{Br}|)^{-1}$, abbreviated as F·(Cl×Br) in the following. A negative value of F·(Cl×Br) corre-

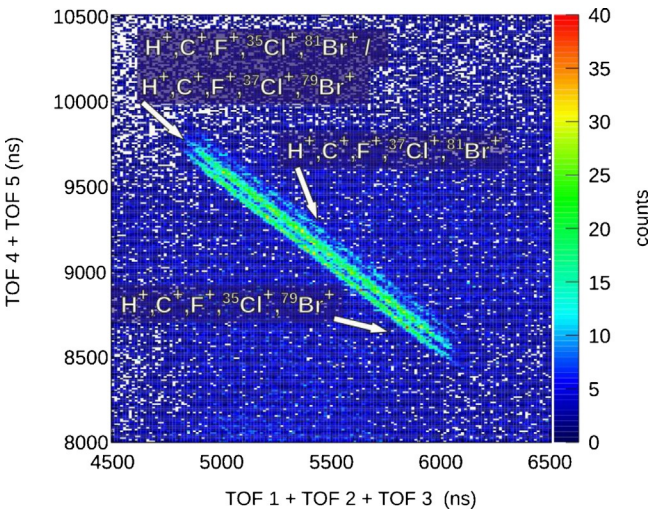

Figure 1. Coincidence spectrum of five measured ions. On the *x*-axis, the sum of the times-of-flight for the first three detected ions is plotted, on the *y*-axis the sum of the times-of-flight of the fourth and fifth ion. Ions from a Coulomb explosion yield a line in this representation due to linear momentum conservation. The substructure originates from the different isotopes of chlorine and bromine.

© 2016 Wiley-VCH Verlag GmbH & Co. KGaA, Weinheim

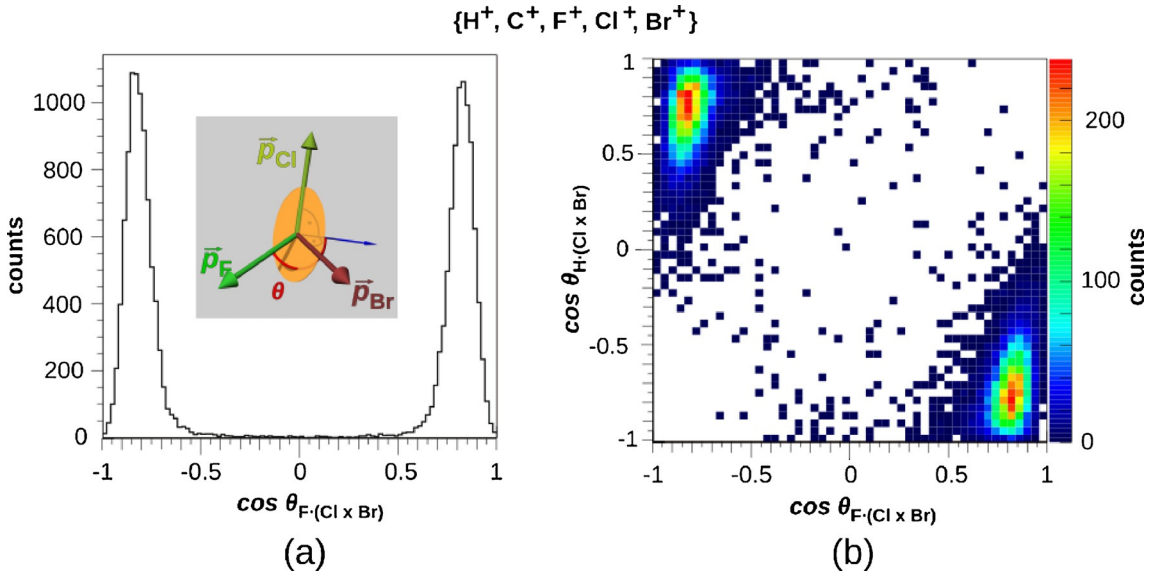

Figure 2. Chirality parameter cos θ for the fragmentation of CHBrClF into five singly charged atomic ions. The geometric definition of the angle θ is given in the inset. The two peaks in (a) indicate a clear separation of enantiomers. The correlation diagram (b) of the two triple products F·(Cl×Br) and H·(Cl×Br) demonstrates the consistency for almost all events.

sponds to an *S*-type arrangement of the momenta in the Cahn–Ingold–Prelog nomenclature[19] whereas a positive value corresponds to an *R*-type arrangement.

Figure 2b shows a correlation diagram of the triple products F·(Cl×Br) and H·(Cl×Br). The position of the peaks on the negative diagonal demonstrates that the assignment of absolute configuration is consistent for the proton and the fluorine ion: For events where a positive value of F·(Cl×Br) indicates an *R*-type molecule, the corresponding value for H·(Cl×Br) is negative. Proton migration to the other side of the carbon atom during the ionization process can thus be ruled out.

In our previous experiments on laser ionization, the linear momentum distribution of the light proton nevertheless proved to be rather broad. Figure 3 compares the triple product H·(Cl×Br) of the synchrotron experiment with the data set obtained with the laser. Despite the small number of events in the latter case, an improvement can clearly be seen. We attribute this to the typical Auger decay times being significantly below 10 fs whereas the laser pulse width was determined as 40 fs.

The three-dimensional representation of the linear momenta in the molecular frame of reference (Figure 4) confirms the

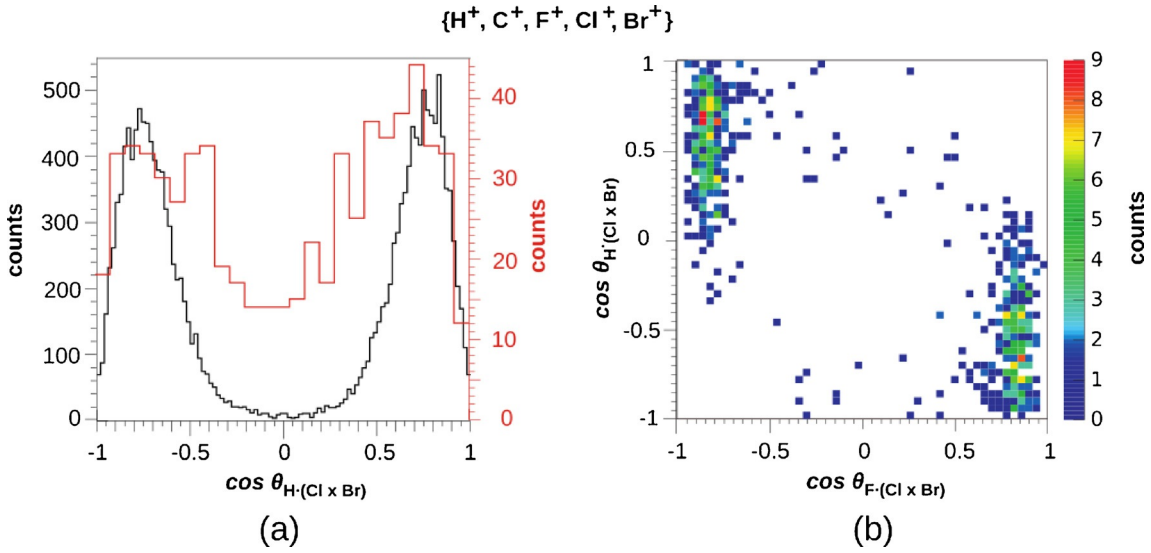

Figure 3. a) Comparison of the triple product H·(Cl×Br) for the laser experiment,[2] shown in red and the synchrotron experiment (black). The smaller spread in the synchrotron experiment is attributed to a faster ionization process, preventing broadening of the distribution due to proton motion. b) Correlation diagram for the laser ionization, in analogy to Figure 2(b), shows that this broadening does not lead to ambiguities in the assignment of enantiomers.

© 2016 Wiley-VCH Verlag GmbH & Co. KGaA, Weinheim

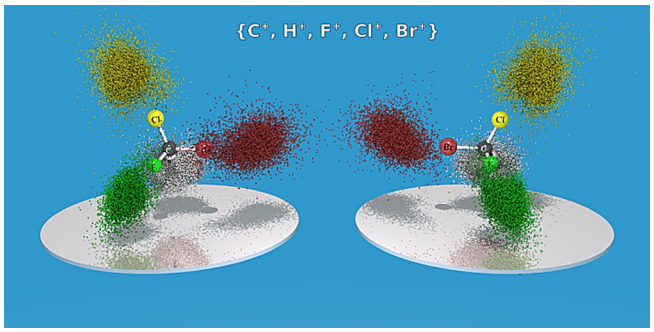

Figure 4. Three-dimensional representation of the linear momenta in the molecular frame for the fragmentation into five atomic ions, overlayed with a structure model. Color codes are white: H; black: C; green: F; yellow: Cl; red: Br. Transformation into the molecular frame is described in the Supporting Information.

good separation of enantiomers, suggesting an unambiguous assignment of absolute configuration on the level of individual molecules. The transformation into the molecular frame is described in the Supporting Information.

2.3. Partial Fragmentation into Molecular Ions

As can be seen from the definition of the chirality parameter, only three linearly independent momentum vectors are needed to determine the handedness of the system. It follows that the complete break-up of the molecule into atomic ions is not a prerequisite for the assignment of absolute configuration. Fragmentation pathways including molecular ions can thus be used to achieve this goal. This fact is of particular interest for the study of larger molecules where complete fragmentation cannot be expected.

In the case of CHBrClF, it is an obvious choice to investigate break-ups including a CX^+-fragment with X being H, F, Cl or Br. From these four possibilities, the fragmentation pathways with the ions {CF^+, H^+, Cl^+, Br^+} (channel **II**) and {CH^+, F^+, Cl^+, Br^+} (channel **III**) were found in the recorded data.

Figure 5 shows the triple products for different break-ups. While the assignment of absolute configuration works well with CH^+, the fragmentation channel **II** containing CF^+ barely allows to distinguish enantiomers. The graphs for **II** show that $\cos\theta_{H\cdot(Cl\times Br)}$ has a broad distribution and that $\cos\theta_{CF\cdot(Cl\times Br)}$ has two overlapping peaks close to 0, indicating that these three linear momenta are nearly coplanar due to the small linear momentum carried away by the proton.

As the detection probability for the cations is significantly lower than 100% (see Experimental Section), the detection efficiency is expected to be higher for the coincident measurement of four ions instead of five. Table 1, however, demonstrates that the yield in the case of the partial fragmentation

Table 1. Total ion yields for different fragmentation channels in the synchrotron experiment. Reaction products in square brackets remained undetected (see Section 3.4 for details). Whereas fragmentation into molecular ions does not increase the yield (channels II and III) significantly, the incompletely detected break-ups show a significantly higher efficiency. For channel III, an overlap with the pathway $[H]^{+,0}+\{C^+, F^+, Cl^+, Br^+\}$ cannot be eliminated completely.

	Fragmentation pathway	Yield (events)
I	$CHBrClF^{5+}\rightarrow\{C^+, H^+, F^+, Cl^+, Br^+\}$	4.7×10^4
II	$CHBrClF^{4+}\rightarrow\{CF^+, H^+, Cl^+, Br^+\}$	2.0×10^4
III	$CHBrClF^{4+}\rightarrow\{CH^+, F^+, Cl^+, Br^+\}$	1.1×10^5
IV	$CHBrClF^{5+,4+}\rightarrow[Br]^{+,0}+\{C^+, H^+, F^+, Cl^+\}$	5.9×10^5
V	$CHBrClF^{5+,4+}\rightarrow[F]^{+,0}+\{C^+, H^+, Cl^+, Br^+\}$	3.4×10^5
VI	$CHBrClF^{5+,4+}\rightarrow[C]^{+,0}+\{H^+, F^+, Cl^+, Br^+\}$	3.6×10^5
VII	$CHBrClF^{5+,4+,3+}\rightarrow[H,Br]^{2+,+,0}+\{C^+, F^+, Cl^+\}$	2.2×10^6
VIII	$CHBrClF^{5+,4+,3+}\rightarrow[H,Cl]^{2+,+,0}+\{C^+, F^+, Br^+\}$	1.1×10^6
IX	$CHBrClF^{5+,4+,3+}\rightarrow[C,F]^{2+,+,0}+\{H^+, Cl^+, Br^+\}$	1.5×10^6

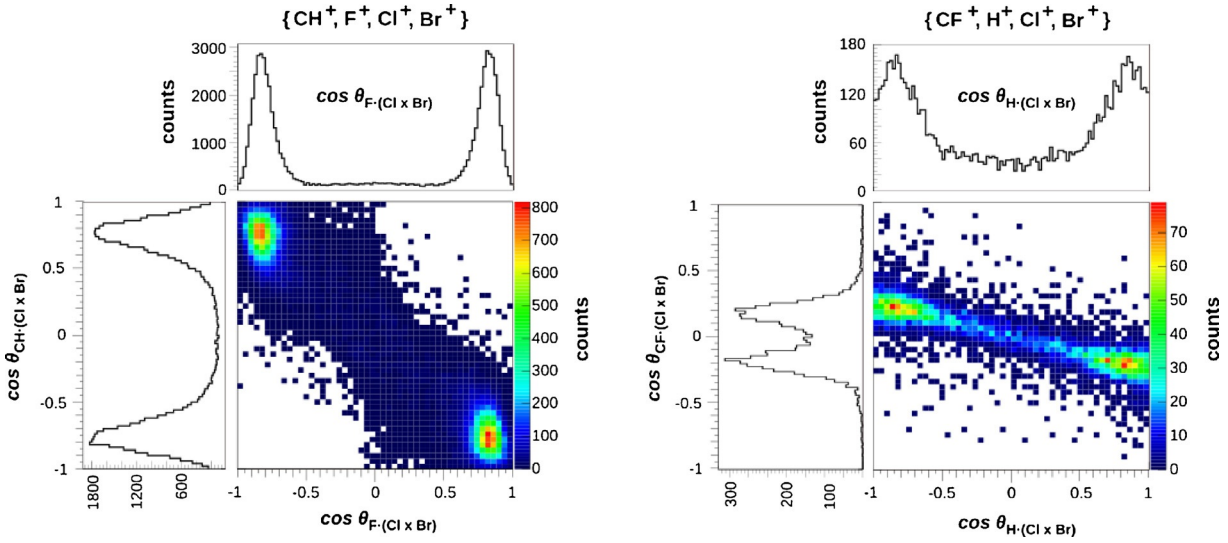

Figure 5. Triple products for fragmentation pathways including molecular ions, in analogy to Figure 2. The fragmentation into {CH^+, F^+, Cl^+, Br^+} promises a good separation of enantiomers (left), despite a small background (see text). For the break-up into {CF^+, H^+, Cl^+, Br^+}, the separation is less clear, as the fragments CF^+, Cl^+ and Br^+ are nearly coplanar (right).

© 2016 Wiley-VCH Verlag GmbH & Co. KGaA, Weinheim

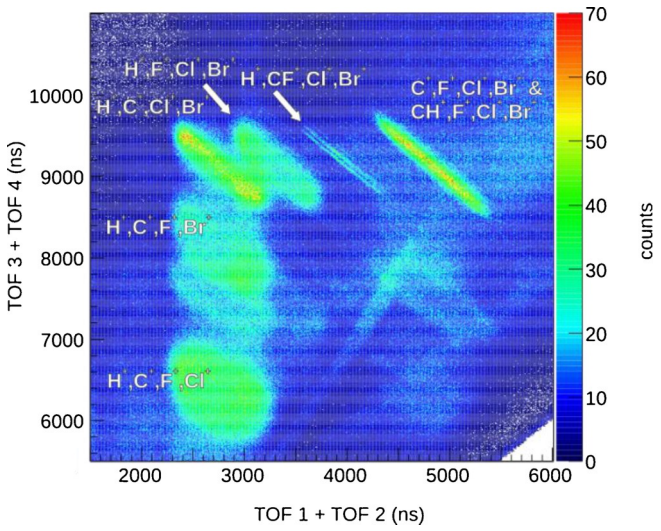

Figure 6. Coincidence plot for the identification of fragmentation channels. On the *x*-axis, the sum of the time-of-flight of the first and second ion is plotted; the *y*-axis displays the corresponding sum of the third and fourth ion. Fragmentation channels in which the detected ions have zero-sum momentum show up as narrow lines. Fragmentations with a neutral product are spread out in the plot due to the neutral particle's linear momentum. Different fragmentation pathways are identified from the ions' times-of-flight.

into four ions is not higher than in the case of complete fragmentation. Similar results for partial break-ups were extracted from the laser measurement,[2] and are shown in the Supporting Information.

2.4. Incomplete Detection of Ionic Fragments

Looking at the raw four-ion coincidence spectra (Figure 6), various features can be identified that correspond to fragmentation pathways with one of the fragment masses missing. Two possibilities contribute to this scenario: either a neutral dissociation product is involved or a charged fragment was not detected due to the limited detection efficiency of the setup (Experimental Section). As shown in Table 1, the yield for these break-up channels is considerably higher than for the channels investigated before. It is thus worthwhile to check if they can also be used to determine absolute configuration.

As one of the fragments is not detected, the linear momenta of the detected ions do not sum up to 0 as in the previous cases. Instead, the sum momentum is attributed to the missing fragment. To suppress some background, the linear momentum vectors of the detected ions and of the missing fragment are required to be smaller than the maximum linear momentum of the respective fragment in the case of the complete break-up.

Figure 7 shows reconstructed linear momenta for several fragmentation pathways, compared to the measured linear momenta for the fragmentation into five singly charged ions. The broadening of the distribution has several sources: Firstly, different fragmentation pathways can lead to the same observed reaction products. This is particularly evident for the undetected fluorine (Figure 7, middle). The shoulder at higher linear momentum values corresponds to the values of the fluorine linear momentum that is observed for the break-up into five ions. We conclude that this part of the distribution is caused by actual break-ups into five atomic ions for which the fluorine cation was not detected. Comparison of the values of the kinetic energy release (KER) for these events and the five-ion fragmentation supports this explanation. Secondly, the broadening is caused by the fact that background cannot be reduced as effectively because the sum momentum check cannot be applied as stringently. Thirdly, the isotopic mass of the detected fragments Cl^+ or Br^+ cannot be determined because the linear momentum distributions of the different isotopes overlap. For the calculation of linear momenta from the raw data, the mass of the lighter isotope was assumed, leading to an error of about 20 atomic units of linear momentum for the molecules containing the heavy isotope. This value, however, is not rooted in physical properties of the molecule but in the experimental parameters (Experimental Section).

Figure 8 (top row) shows triple products for different fragmentation pathways. A separation of the two enantiomers is clearly visible and the overall consistency can be demonstrated using different triple products (bottom row). The background is significantly higher than in the case where all fragments

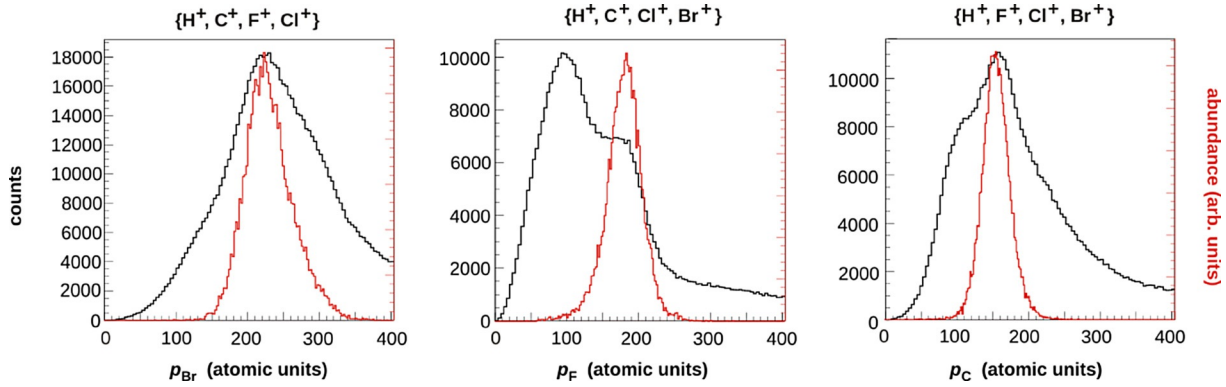

Figure 7. Distribution of reconstructed linear momenta (black) for different fragmentation pathways. The measured ions are given on top; their sum momentum is attributed to the missing mass. For comparison, the linear momentum distribution of the respective ion in the complete fragmentation is displayed (red).

© 2016 Wiley-VCH Verlag GmbH & Co. KGaA, Weinheim

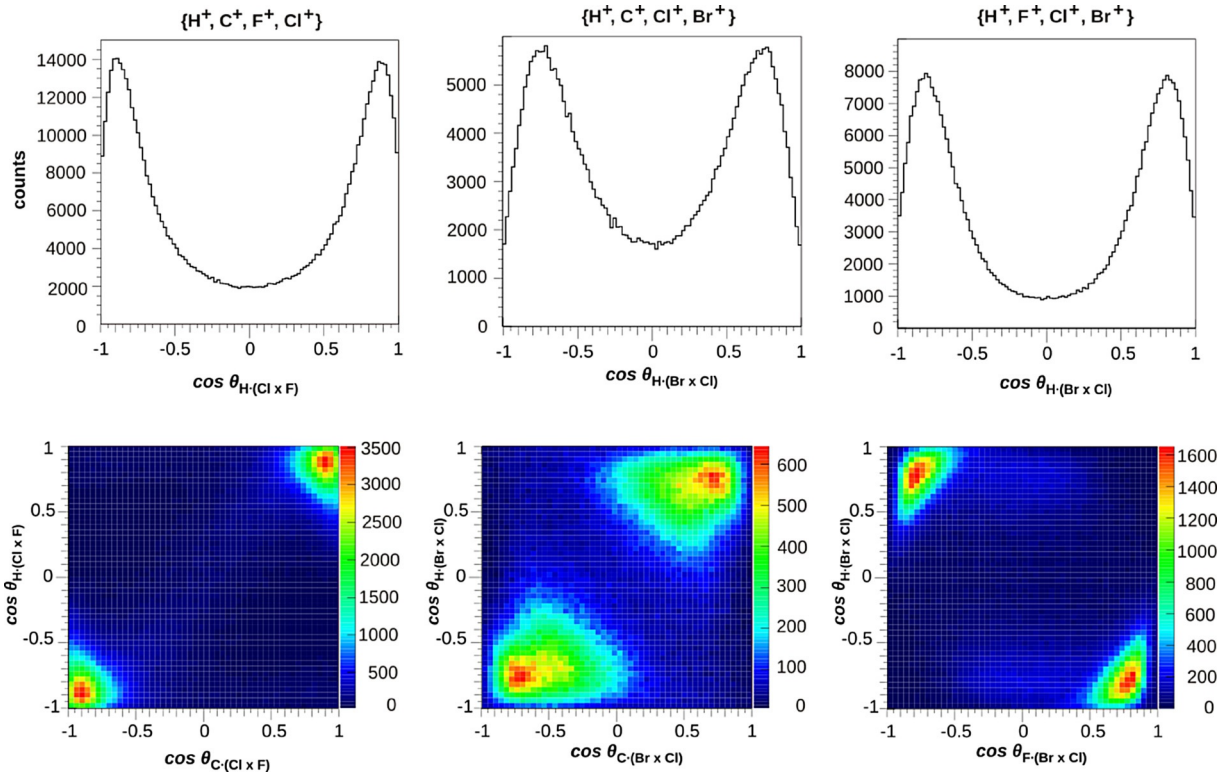

Figure 8. Separation of enantiomers using different fragmentation pathways with one fragment being undetected. The measured fragments are given on top of the column. The top row shows the triple products as defined in the text, the bottom row displays the correlation of two triple products. As is expected from a classical simulation, linear momenta of H^+ and C^+ point in the same direction, resulting in maxima on the main diagonal.

were detected. Contrary to the complete fragmentation, the assignment of absolute configuration is thus not certain on a singe-molecule level anymore.

In order to evaluate how reliable the assignment of enantiomers is, the consistency of seven possible triple products was checked (Table 2 in the Supporting Information). For the fragmentation pathways **IV** and **V**, about 75% of the events show a consistent sign of all seven triple products; for pathway **VI** with detected {H^+, F^+, Cl^+, Br^+}, the consistency lies below 20%. This discrepancy is supposedly due to the multiplicity of (sequential) pathways in which a neutral carbon atom can be ejected during Coulomb explosion.

The events with consistent sign were used to estimate the influence of the unknown isotopic composition of the individual molecules. To do so, linear momenta were calculated for all isotopic combinations of chlorine and bromine isotopes, and the resulting signs of triple products were compared (see Table 3 in the Supporting Information). For every isotopic combination, more than 90% of the events still showed consistency, meaning that for these events, the unknown isotopic composition does not affect the correct assignment of handedness. This value could probably be increased with an improved spectrometer.

In analogy, events with only three detected particles could as well be used to determine handedness, provided an undetected fragment is involved (if this were not the case, all linear momenta would be coplanar due to linear momentum conservation, and thus insufficient to determine the handedness).

Figure 9a shows that the background is even higher than in the four-particle case. As only one triple product can be calculated, the possibility of cross-checks as in the previous cases is lost. Assignment of handedness must thus be taken with caution as rearrangement during the fragmentation process cannot be excluded. Quantum chemical calculations reveal existence of a metastable planar isomer of the CHBrClF trication, which implies a concomitant loss of structural information in CEI. Even for small fragment dications such as $CHBr^{2+}$, isomers are known to exist[20] (see also the review[21] on (meta)stable highly charged molecular ions). Nevertheless, the two distinct peaks at same absolute value indicate a good separation of enantiomers for the fragmentation channels shown here, and the three-dimensional representation for the *R*-enantiomer in the molecular frame (Figure 9b) confirms this finding. Analogue plots for additional break-up channels can be found in the Supporting Information.

3. Conclusions

In this contribution we showed that a single X-ray photon from a synchrotron source can be used to induce multiple fragmentation of the chiral prototype CHBrClF, allowing determination of absolute configuration.

Taking literature on multiple photoionization of noble gas atoms[22,23] into account, we conclude that mostly initial holes in the bromine M-shell and chlorine L-shell contribute to the fragmentation into five and four ions. In order to achieve such

© 2016 Wiley-VCH Verlag GmbH & Co. KGaA, Weinheim

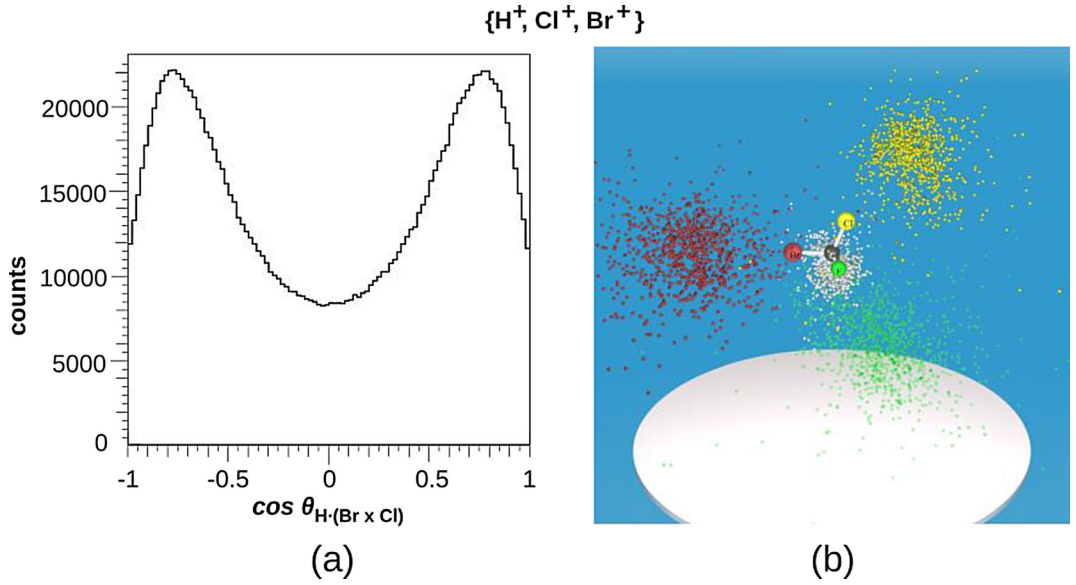

Figure 9. Fragmentation pathway with three detected ions H^+, Cl^+, Br^+. The triple product H·(Br×Cl) indicates a separation of enantiomers (a), albeit only on a statistical level. The three-dimensional distribution of linear momenta in the molecular frame (b) for the *R*-enantiomer confirms the separation. The reconstructed momentum is attributed to fluorine as indicated by the semi-transparent color. Several outliers are also visible. For better visibility, only 1000 events are shown. The transformation into the molecular frame of reference is described in the Supporting Information.

high charge states in organic molecules with only light atoms, energies well above the fluorine 1s state (or respectively carbon 1s or oxygen 1s states in the case of non-halogenated species) seem to be most promising. As work on multiple ionization of neon shows, the probability for quadruple ionization still increases several hundred eV above the neon 1s threshold, due to double core hole excitation[22] or to direct double ionization.[23]

With the photon energy chosen in the present case (710 eV), the efficiency for fragmentation into five singly charged ions was significantly increased compared to previous laser experiments. Moreover, the proton's linear momentum distribution was not as broad as in the latter case, presumably due to faster ionization and fragmentation processes.

Investigation of fragmentation pathways containing the molecular ions CH^+ and CF^+ shows that these channels can be used for the determination of absolute configuration as well. Although efficiency is not increased, this approach seems promising for more complex molecules for which complete fragmentation cannot be achieved anymore.

A significant increase in efficiency is obtained in cases where one of the fragments is not detected. When four atomic ions are collected and one atom is missing, the determination of handedness is still very reliable on a statistical level, and use of different fragments shows consistent assignment of enantiomers. The non-vanishing background, however, leaves an uncertainty in the enantiomeric determination of *individual* molecules. When only three ions are detected, a separation of enantiomers is possible, and efficiency is increased significantly. Together with a more detailed investigation of the fragmentation dynamics, these fragmentation pathways can thus be used to determine the absolute configuration of a sample.

Experimental Section

Measurements were performed with the COLTRIMS-technique that has been described in detail elsewhere.[11,24] The vapor pressure of the sample at room temperature was used to form a supersonic jet by expanding the gas through a 30 µm nozzle into a vacuum chamber. The jet is collimated by two skimmers (300 µm in diameter) and at right angle intersected with a femtosecond laser beam or synchrotron radiation.

The results presented here were obtained at the undulator beamline SEXTANTS[25] of the synchrotron SOLEIL in St. Aubin, France, with a photon energy of 710 eV. For this experiment, the racemic sample of CHBrClF was prepared as described by Swarts[26] via fluorination of $CHBr_2Cl$ with SbF_3 in presence of Br_2. If one considers atomic cross section data, the major contributions to ionization at this energy are expected to stem from the F(1s) state (23%), 21% from Br(3d), 18% from Br(3p) and 15% from Cl(2p) (see Table 1 in the Supporting Information). Formation of double core hole states from C(1s) ionization is considerably less likely, but expected to induce fast formation of higher charge states that are favorable in multiple fragmentation (see for example Ref. [27] for results on the parent compound methane).

Contrary to the laser experiment (Ref. [2] and the Supporting Information herein), lighter elements present in the residual gas are hardly ionized by synchrotron radiation which leads to a lower background signal.

After ionization, positive ions and electrons are separated by the homogeneous electric field of a time-of-flight (TOF) spectrometer. In the measurements presented here, electrons are not considered. Cations are guided onto a time- and position-sensitive detector. The ionic species can be identified because the square root of the mass-to-charge-ratio is proportional to the time-of-flight in an electric field of strength *E*. Contrary to conventional mass spectrometry, the electric field and the length of the spectrometer are tuned in such a way that linear momentum information can be retrieved

© 2016 Wiley-VCH Verlag GmbH & Co. KGaA, Weinheim

from the spread in time-of-flight. In the direction perpendicular to the TOF-axis, ions propagate with the velocity they gain from Coulomb explosion. Linear momenta in all three dimensions can then simply be calculated with the known time-of-flight and impact position on the detector. It should be noted that the effect of the linear momentum spread on the time-of-flight width decreases linearly with increasing field strength E while the separation of the masses decreases only with the square root of the field strength. A compromise between good mass resolution and good linear momentum resolution must thus be found. In the case of complete detection of all fragmentation products, different isotopes can then be separated by virtue of linear momentum conservation. This is not possible for incomplete detection of the fragments. Assuming the wrong isotope will result in an error in the calculated linear momentum; this error will aggravate with higher spectrometer field because the same mass difference corresponds to a bigger linear momentum difference than in case of a low electric field.

When performing multi-hit coincidences, the limited efficiency of the detector severely affects data acquisition rates. Depending on the mass we estimate an efficiency per ion in the order of 20% to 50% for 2 keV ion kinetic energy at impact on the MCP,[28] resulting in a probability of less than 4% to actually record a five-particle event and even lower probabilities for detecting complete breakups of larger molecules.

Acknowledgements

We gratefully acknowledge help from and discussion with Timur Isaev, Alexander Schießer, Guido Grassi, Julia Kiedrowski and Michael Reggelin. The experiments were performed at SOLEIL synchrotron (France) at the SEXTANTS beam line with the approval of the Soleil Peer Review Committee (Project No. 20130255 and 20140056). We are grateful to N. Jaouen for his help during the measurements as well as the SOLEIL staff for stable operation of the storage ring during the experiments. Sebastian Marquardt thanks the Fonds der Chemischen Industrie and Sabrina Marquardt thanks the Deutsche Studienstiftung for a scholarship. Markus Schöffler acknowledges support by the Adolf Messer foundation. This work was supported by the State Initiative for the Development of Scientific and Economic Excellence (LOEWE) in the LOEWE focus ELCH and the German Federal Ministry of Education and Research (BMBF).

Keywords: absolute configuration · chirality · cold target recoil ion momentum spectroscopy · Coulomb explosion imaging · synchrotron radiation

[1] J. Bijvoet, A. Peerdeman, A. van Bommel, *Nature* **1951**, *168*, 271 – 272.
[2] M. Pitzer, M. Kunitski, A. Johnson, T. Jahnke, H. Sann, F. Sturm, L. Schmidt, H. Schmidt-Böcking, R. Dörner, J. Stohner, J. Kiedrowski, M. Reggelin, S. Marquardt, A. Schießer, R. Berger, M. Schöffler, *Science* **2013**, *341*, 1096 – 1100.
[3] P. Herwig, K. Zawatzky, M. Grieser, O. Heber, B. Jordon-Thaden, C. Krantz, O. Novotný, R. Repnow, V. Schurig, D. Schwalm, Z. Vager, A. Wolf, O. Trapp, H. Kreckel, *Science* **2013**, *342*, 1084 – 1086.
[4] Z. Vager, R. Naaman, E. Kanter, *Science* **1989**, *244*, 426 – 431.
[5] L. P. H. Schmidt, T. Jahnke, A. Czasch, M. Schöffler, H. Schmidt-Böcking, R. Dörner, *Phys. Rev. Lett.* **2012**, *108*, 073202.
[6] M. Kunitski, S. Zeller, J. Voigtsberger, A. Kalinin, L. P. H. Schmidt, M. Schöffler, A. Czasch, W. Schöllkopf, R. E. Grisenti, T. Jahnke, D. Blume, R. Dörner, *Science* **2015**, *348*, 551.
[7] J. Voigtsberger, S. Zeller, J. Becht, N. Neumann, F. Sturm, H.-K. Kim, M. Waitz, F. Trinter, M. Kunitski, A. Kalinin, J. Wu, W. Schöllkopf, D. Bressanini, A. Czasch, J. B. Williams, K. Ullmann-Pfleger, L. P. H. Schmidt, M. S. Schöffler, R. E. Grisenti, T. Jahnke, R. Dörner, *Nat. Commun.* **2014**, *5*, 5765.
[8] Z. Vager, E. Kanter, G. Both, P. Cooney, A. Faibis, W. Koenig, B. Zabransky, D. Zajfman, *Phys. Rev. Lett.* **1986**, *57*, 2793 – 2795.
[9] T. Kitamura, T. Nishide, H. Shiromaru, Y. Achiba, N. Kobayashi, *J. Chem. Phys.* **2001**, *115*, 5 – 6.
[10] P. Herwig, K. Zawatzky, D. Schwalm, M. Grieser, O. Heber, B. Jordon-Thaden, C. Krantz, O. Novotný, R. Repnow, V. Schurig, Z. Vager, A. Wolf, O. Trapp, H. Kreckel, *Phys. Rev. A* **2014**, *90*, 052503.
[11] R. Dörner, V. Mergel, O. Jagutzki, L. Spielberger, J. Ullrich, R. Moshammer, H. Schmidt-Böcking, *Phys. Rep.* **2000**, *330*, 95 – 192.
[12] J. Yeh, I. Lindau, *Atom. Data Nucl. Data* **1985**, *32*, 1 – 155.
[13] V. Jonauskas, S. Kuas, R. Karazija, *Phys. Rev. A* **2011**, *84*, 053415.
[14] T. Carlson, W. Hunt, M. Krause, *Phys. Rev.* **1966**, *151*, 41 – 47.
[15] S. Brünken, C. Gerth, B. Kanngießer, T. Luhmann, M. Richter, P. Zimmermann, *Phys. Rev. A* **2002**, *65*, 042708.
[16] B. Erk, D. Rolles, L. Foucar, B. Rudek, S. W. Epp, M. Cryle, C. Bostedt, S. Schorb, J. Bozek, A. Rouzee, A. Hundertmark, T. Marchenko, M. Simon, F. Filsinger, L. Christensen, S. De, S. Trippel, J. Küpper, H. Stapelfeldt, S. Wada, K. Ueda, M. Swiggers, M. Messerschmidt, C. D. Schröter, R. Moshammer, I. Schlichting, J. Ullrich, A. Rudenko, *Phys. Rev. Lett.* **2013**, *110*, 053003.
[17] A. Knapp, A. Kheifets, I. Bray, T. Weber, A. L. Landers, S. Schössler, T. Jahnke, J. Nickles, S. Kammer, O. Jagutzki, L. P. Schmidt, T. Osipov, J. Rösch, M. H. Prior, H. Schmidt-Böcking, C. L. Cocke, R. Dörner, *Phys. Rev. Lett.* **2002**, *89*, 033004.
[18] K. Kreidi, D. Akoury, T. Jahnke, T. Weber, A. Staudte, M. Schöffler, N. Neumann, J. Titze, L. P. H. Schmidt, A. Czasch, O. Jagutzki, R. A. C. Fraga, R. E. Grisenti, M. Smolarski, P. Ranitovic, C. L. Cocke, T. Osipov, H. Adaniya, J. C. Thompson, M. H. Prior, A. Belkacem, A. L. Landers, H. Schmidt-Böcking, R. Dörner, *Phys. Rev. Lett.* **2008**, *100*, 133005.
[19] R. S. Cahn, C. Ingold, V. Prelog, *Angew. Chem. Int. Ed.* **1966**, *5*, 385 – 415.
[20] J. Roithová, J. Zabka, Z. Herman, R. Thissen, D. Schröder, H. Schwarz, *J. Phys. Chem. A* **2006**, *110*, 6447 – 6453.
[21] D. Schröder, H. Schwarz, *J. Phys. Chem. A* **1999**, *103*, 7385 – 7394.
[22] N. Saito, I. Suzuki, *Phys. Scr.* **1994**, *49*, 80 – 85.
[23] T. Carlson, M. Krause, *Phys. Rev.* **1965**, *140*, 1057 – 1064.
[24] J. Ullrich, R. Moshammer, A. Dorn, R. Dörner, L. Schmidt, H. Schmidt-Böcking, *Rep. Prog. Phys.* **2003**, *66*, 1463 – 1545.
[25] M. Sacchi, N. Jaouen, H. Popescu, R. Gaudemer, J. M. Tonnerre, S. G. Chiuzbaian, C. F. Hague, A. Delmotte, J. M. Dubuisson, G. Cauchon, B. Lagarde, F. Polack, *J. Phys. Conf. Ser.* **2013**, *425*, 072018.
[26] F. Swarts, *Bull. Acad. R. Belg.* **1893**, *26*, 102 – 106.
[27] J. H. D. Eland, M. Tashiro, P. Linusson, M. Ehara, K. Ueda, R. Feifel, *Phys. Rev. Lett.* **2010**, *105*, 213005.
[28] M. Krems, J. Zirbel, M. Thomason, R. D. DuBois, *Rev. Sci. Instrum.* **2005**, *76*, 093305.

Manuscript received: December 5, 2015
Final Article published: June 14, 2016

© 2016 Wiley-VCH Verlag GmbH & Co. KGaA, Weinheim